SUPPLEMENTARY MATERIAL

Dynamic alterations of rat nucleus accumbens dendritic spines over two months of abstinence from extended-access cocaine self-administration

Daniel T. Christian, Ph.D.*, Xiaoting Wang, Ph.D.*, Eugenia L. Chen, M.S., Lakshya K. Sehgal, M.S., Michael N. Ghassemlou, M.S., Julia J. Miao, M.S., Derenik Estepanian, M.S., Cameron H. Araghi, M.S., Grace E. Stutzmann, Ph.D., Marina E. Wolf, Ph.D.

Department of Neuroscience, The Chicago Medical School at Rosalind Franklin University of Medicine and Science, North Chicago, IL 60064, USA; *These authors contributed equally to this work.

Contents:

SUPPLEMENTARY METHODS

Microinjection of Lucifer yellow

A 5% (100 mM) Lucifer yellow solution (Invitrogen, Carlsbad, CA) was injected into medium spiny neurons (MSNs) using an iontophoretic cell loading procedure similar to that described previously (Meredith *et al*, 1992; Dumitriu *et al*, 2011). Briefly, coronal brain slices (200uM thick) were floated in 1X PBS in a glass petri dish with a clear microscope slide glued to the bottom. Slice position was secured by placing a piece of nitrocellulose membrane, with a hole cut out, over the slice and securing the membrane with metal washers. Glass capillary tubes were pulled into sharp electrodes and filled with Lucifer yellow solution. Ultraviolet illumination was used to visualize the Lucifer Yellow filled electrode under 4x magnification. Electrodes were placed into the tissue and systematically moved on a diagonal through the thickness of the brain slice. Once a cell membrane was pierced, the Lucifer yellow solution passively filled the cell body and the proximal dendritic arbor, allowing visualization of the cell. Injection of constant negative current (1–5 nA) was then delivered to robustly fill the entire dendritic arbor. Electrical current was ceased at the first sign of Lucifer Yellow leak from the injection site (typically 1-3 min) and the electrode was removed from the cell body. Single electrodes were re-used to fill multiple cells throughout the brain region of interest bilaterally. Wide spacing between filled neurons was kept so that no overlap of filled dendritic arbors could be observed. Sections with Lucifer yellow filled cells were then mounted in Vectashield (Vector Laboratories, Burlingame, CA) on slides with a 120 µm spacer (Electron Microscopy Sciences, Hatfield, PA), cover-slipped, and sealed with nail polish before imaging. All slides were stored at 4^{o}C in light sealed slide boxes.

Confocal imaging and spine analysis

Coronal sections with Lucifer yellow filled neurons were first imaged under 10x magnification to obtain a survey image used for cell numbering and selection (e.g., Figure 1C in main text). Cells selected for

further imaging required a minimum of two dendritic segments that were >50 µm away from the soma and did not overlap with other dendritic branches. These criteria also ensured that we imaged distal dendrites, which show robust cocaine-induced plasticity (Robinson and Kolb, 2004; Ferrario *et al*, 2005). Spine imaging and analysis were then performed as described previously (Dumitriu *et al*, 2011; Dumitriu *et al*, 2012). Images were acquired on a confocal LSM 510 (Carl Zeiss) using a 100X lens (numerical aperture 1.4; Carl Zeiss) and a zoom of 2.5. Pixel size was 0.035 µm in the x–y plane and 0.2 µm in the z plane. Images were taken with a resolution of 1024 X ~300 (the y dimension was adjusted to the particular dendritic segment to expedite imaging), pixel dwell time was 1.58 µm/s, and the line average was set to 4. For each animal (4-5 per group), we analyzed 2-7 dendritic segments per neuron for 6-15 neurons in the NAc core, NAc shell, and the dorsolateral striatum (DLS). All image files were coded to ensure that experimenters were blind to experimental condition during image analysis. Confocal images were then deconvoluted using Huygens Essential software (Scientific Volume Imaging, Netherlands). Quantitative analysis was performed using NeuronStudio (Dumitriu *et al*, 2011; http://research.mssm.edu/cnic/tools-ns.html), which is capable of measuring spine density and automatically classifying spines as thin, mushroom or stubby based on each spine's head to neck diameter ratio, length to head diameter ratio, and head diameter. Analysis settings and classification in NeuronStudio have been validated by comparison to results obtained by trained human operators (Dumitriu *et al*, 2011).

SUPPLEMENTARY TABLE 1

Supplementary Table 1. Analysis of the relationship between average daily cocaine infusions during training and total spine density in the nucleus accumbens core and shell

		Withdrawal Day			
		14	25	36	60
Mean Cocaine Infusions (10 d)		135.33	112.26	121.58	127.12
Core	Mean Total Spine Density	3.84	3.46	4.16	3.28
	Pearson Correlation Coefficient (r)	0.47	-0.73	0.37	0.36
	p value	0.53	0.16	0.63	0.55
Shell	Mean Total Spine Density	3.00	2.78	2.77	2.69
	Pearson Correlation Coefficient (r)	-0.63	-0.77	-0.95	-0.14
	p value	0.37	0.13	**0.05 ***	0.82

For each rat, we determined the average number of daily cocaine infusions over the 10 days of cocaine self-administration training. Pearson correlation coefficients were used to assess the relationship between average daily cocaine infusions and total spine density in the nucleus accumbens core and shell on each withdrawal day.

SUPPLEMENTARY RESULTS AND SUPPLEMENTARY FIGURES 1 AND 2: SPINE DENSITY AND MORPHOLOGY IN THE NUCLEUS ACCUMBENS SHELL

Using the same animals employed for analysis of the NAc core, we examined overall spine density in the NAc shell of saline and cocaine rats at four withdrawal times (Figure S1). On WD14, the total density of dendritic spines did not differ significantly between cocaine and saline groups [Student's t-test, $t(7)=2.02$, $p=0.08$]. There was, however, a significant rightward shift of the cumulative frequency distribution in saline rats compared to cocaine rats, particularly for segments with a high density of spines [Kolmogorov-Smirnov (K-S) test=0.25, $p<0.05$] (Figure S1A). On WD25, saline and cocaine groups did not differ in total spine density [$t(8)=0.24$, $p=0.81$] or the cumulative frequency distribution (K-S test=0.13, $p=0.58$) (Figure S1B). Results at the WD36 time-point also did not demonstrate any significant differences in total spine density [$t(7)=0.75$, $p=0.47$] or the cumulative distribution (K-S test=0.17, $p=0.15$) (Figure S1C). Likewise, no significant group differences were observed on WD60 [total spine density: Student's t-test, $t(8)=0.43$, $p=0.67$; cumulative frequency distribution: K-S test=0.11, $p=0.68$] (Figure S1D).

These results indicate that the cocaine group has a slightly lower density of spines on WD14 compared to the saline group. However, this appears to be driven by a small increase in spine density in the saline group on WD14, relative to other saline withdrawal times, rather than a decrease in spine density in the WD14 cocaine group. Supporting this, ANOVA revealed a significant change in spine density in the NAc shell of saline rats as a function of withdrawal time [$F(3,16)=4.60$, $p<0.05$] and Bonferonni post hoc tests showed relatively more spines in the WD14 saline group compared to the WD25 [$t(16)= 3.31$, $p<0.05$] or WD60 [$t(16)= 3.08$, $p<0.05$] saline groups. There is no obvious explanation for this effect on WD14. Although we cannot rule out a developmental change, we regard this as unlikely since the rats were adults (>P60) at the start of cocaine self-administration. Instead, we believe this is an example of

fluctuations in baseline spine density than can occur from cohort to cohort, as has been found in studies by other groups (e.g., Dumitriu et al, 2012 or Peterson et al, 2015). In contrast to time-dependent changes found in the NAc shell of saline rats, ANOVA revealed no significant change in spine density over withdrawal in the NAc shell of cocaine rats [$F(3,14)=0.7146$, $p=0.55$]. These negative findings for the cocaine group further argue that the saline/cocaine difference on WD14 is attributable to the saline group. It remains possible that modest structural plasticity occurs in the NAc shell of cocaine rats during incubation but is obscured due to greater heterogeneity of cocaine-induced plasticity in NAc shell MSNs compared to NAc core MSNs (see Discussion section in main text). For example, using the present cocaine regimen, all MSNs in the NAc core show CP-AMPAR upregulation, whereas this occurs in only ~50% of NAc shell MSNs (McCutcheon *et al*, 2011).

With these caveats in mind, we proceeded to use automated spine analysis and classification via NeuronStudio to compare spine morphology in the NAc shell of saline and cocaine rats at each withdrawal time (Figure S2). For all withdrawal times, two-way ANOVA (group x spine type) revealed a significant main effect for spine type [WD14: $F(2, 21)=257.10$, $p<0.0001$; WD25: $F(2, 24) = 319.90$, $p < 0.0001$; WD36: $F(2, 21)=223.60$, $p<0.0001$; WD60: $F(2, 21)=223.60$, $p<0.0001$]. As discussed in the main text, this simply reflects the fact that thin spines were more prevalent than other types in all experimental groups.

On WD14, two-way ANOVA also revealed a significant main effect for drug treatment [$F(1,21)=5.15$, $p=0.03$] and a trend towards an interaction between spine type and drug treatment [$F(2, 21)=2.50$, $p = 0.10$]. Post hoc analysis revealed a significantly lower density of thin spines in cocaine rats [Bonferroni, $t(21)=3.015$, $p<0.05$]. As discussed in the second paragraph of Supplementary Results, this finding appears to be driven by an increase in spine density in the saline group. No group differences were

found for stubby spines [Bonferroni, t(21)=1.03, n.s.] or mushroom spines [Bonferroni, t(21)=0.11, n.s.] on WD14 (Figure S2A).

Analysis of WD25 data demonstrated no significant effect of drug treatment [F(1, 24)=0.07, p=0.78] and no significant interaction between spine type and drug treatment [F(2, 24)=0.12, p=0.87]. Post hoc analysis did not reveal a significant group difference for any spine subtype: thin [Bonferroni, t(24)=0.22, n.s.], stubby [Bonferroni, t(24)=0.48, n.s.], or mushroom [Bonferroni, t(24)=0.22, n.s.] (Figure S2B).

Similarly, on WD36 we found no significant effects of drug treatment [F(1, 21)=0.72, p=0.40] and no significant interaction between spine type and drug treatment [F(2, 21)=0.61, p=0.54]. Post hoc analysis did not reveal a significant group difference for any spine subtype: thin [Bonferroni, t(21)=1.13, n.s.], stubby [Bonferroni, t(21)=0.72., n.s.], or mushroom [Bonferroni, t(21)=0.38, n.s.] (Figure S2C).

Results on WD60 were the same as on WD25 and WD36: no significant main effect of drug treatment [F(1, 24)=0.08, p=0.77] and no significant interaction between spine type and drug treatment [F(2, 24)=0.18, p=0.83], along with no significant group difference for thin spines [Bonferroni, t(24)=0.13, n.s.], stubby spines [Bonferroni, t(24)=0.24, n.s.], or mushroom spines [Bonferroni, t(24)=0.61, n.s.] (Figure S2D).

Overall, these results indicate that the small difference in spine density in the NAc shell between saline and cocaine groups on WD14 is attributable to thin spines and most likely to an increase in thin spines in saline rats on WD14 compared to other saline withdrawal times. At the later withdrawal times, we found no differences between saline and cocaine rats in either overall spine density or density of any particular spine subtype.

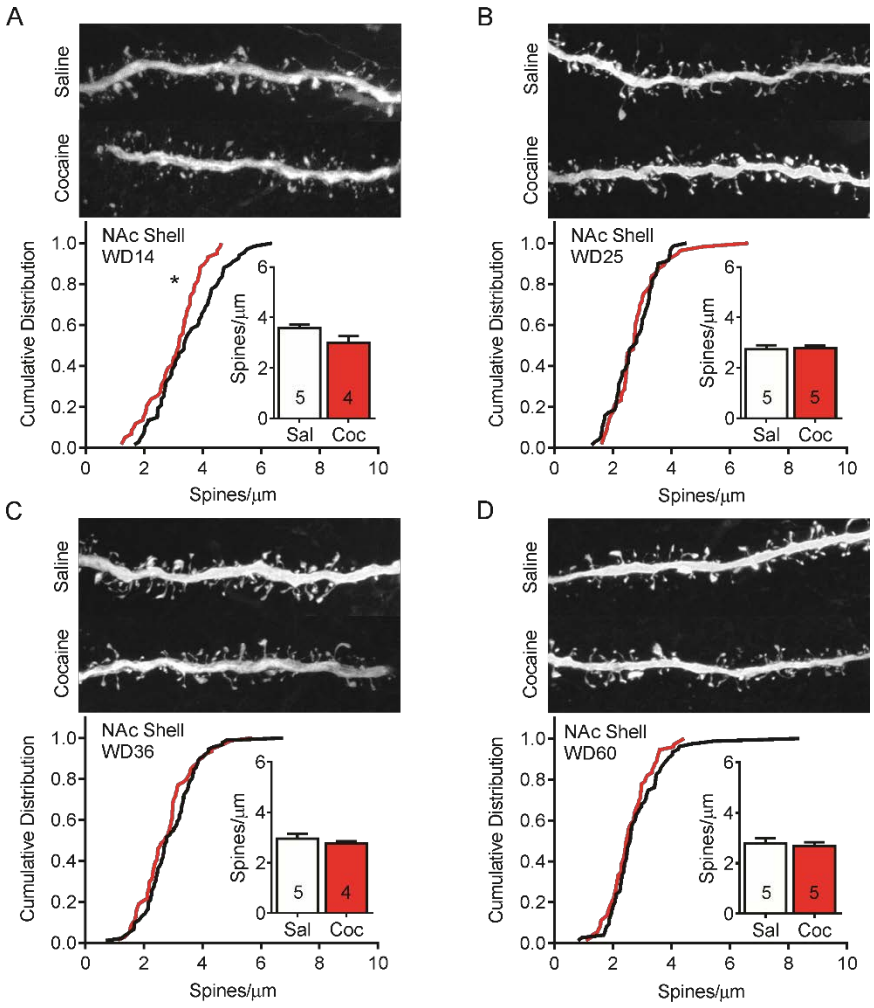

Figure S1. Total spine density in the NAc shell at different withdrawal time-points following extended-access self-administration of saline or cocaine. ***A-D***, Top images show representative projected z-stack images (100x) from each experimental group. Bottom graphs show cumulative distributions for every dendritic segment from all animals in a group (black line = saline, red line = cocaine). Inset graphs present mean total spine density averaged first by animal and then for the group. Numbers in bars represent the number of animals in each condition. ***A***, Total spine density did not differ significantly between cocaine and saline animals on withdrawal day (WD) 14. However, the saline and cocaine groups exhibited a significant difference in the cumulative frequency distribution. This appears to be driven by a small increase in spine density in the saline group on WD14 compared to saline groups on other WDs (see spine density values for the saline groups in the inset bar graphs and statistical analyses presented in Supplementary Results). ***B-D***, No group differences in total spine density or the cumulative distribution were found on WD25, WD36, or WD60. *$p < 0.05$

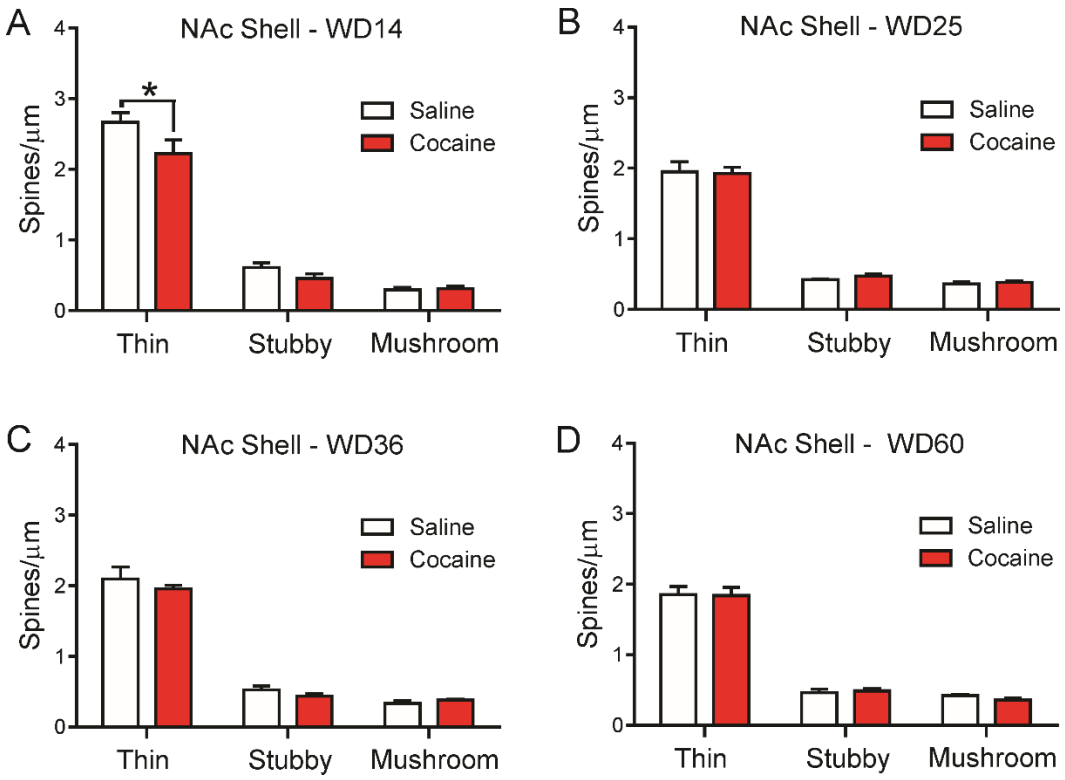

Figure S2. Density of thin, stubby and mushroom spines in the NAc shell at different withdrawal time-points following extended-access self-administration of saline or cocaine. ***A***, On withdrawal day (WD) 14, the density of thin spines was relatively lower in the cocaine group. This difference appears to be driven by an increase in thin spine density in the saline group on WD14 (compare thin spine density in saline groups at different withdrawal times). This change in thin spines likely underlies the leftward shift in total spine density exhibited by the WD14 saline group in **Figure S1A**. ***B-D***, The density of dendritic spine subtypes did not differ between saline and cocaine groups on WD25, WD36, or WD60, consistent with no alterations in total spine density measures after these withdrawal periods. *$p < 0.05$

SUPPLEMENTARY REFERENCES

Dumitriu D, Laplant Q, Grossman YS, Dias C, Janssen WG, Russo SJ, et al (2012). Subregional, dendritic compartment, and spine subtype specificity in cocaine regulation of dendritic spines in the nucleus accumbens. *J Neurosci* **32**(20): 6957-6966.

Dumitriu D, Rodriguez A, Morrison JH (2011). High-throughput, detailed, cell-specific neuroanatomy of dendritic spines using microinjection and confocal microscopy. *Nat Protocols* **6**(9): 1391-1411.

Ferrario CR, Gorny G, Crombag HS, Li Y, Kolb B, Robinson TE (2005). Neural and behavioral plasticity associated with the transition from controlled to escalated cocaine use. *Biol Psychiatry* **58**(9): 751-759.

McCutcheon JE, Wang X, Tseng KY, Wolf ME, Marinelli M (2011). Calcium-permeable AMPA receptors are present in nucleus accumbens synapses after prolonged withdrawal from cocaine self-administration but not experimenter-administered cocaine. *J Neurosci* **31**(15): 5737-5743.

Meredith GE, Agolia R, Arts MPM, Groenewegen HJ, Zahm DS (1992). Morphological differences between projection neurons of the core and shell in the nucleus accumbens of the rat. *Neuroscience* **50**(1): 149-162.

Peterson BM, Mermelstein PG, Meisel RL (2015). Estradiol mediates dendritic spine plasticity in the nucleus accumbens core through activation of mGluR5. *Brain Struct Funct* **220**(4): 2415-2422.

Robinson TE, Kolb B (2004). Structural plasticity associated with exposure to drugs of abuse. *Neuropharmacology* **47** Suppl 1: 33-46.